Steady State Free Precession (SSFP) and fMRI: Expressions Accounting for Reversible vs Irreversible Transverse Relaxation Effects

Robert V. Mulkern[1], Mukund Balasubramanian[1], Dimitrios Mitsouras[2], and Stephen Haker[2]

[1]*Department of Radiology, Children's Hospital Boston, Boston, Massachusetts, United States,* [2]*Department of Radiology, Brigham and Women's Hospital, Boston, Massachusetts, United States*

Introduction: SSFP offers an intriguing alternative to echo planar imaging (EPI) methods for performing fMRI (1-3). High resolution, high SNR images with minimal spatial distortion may be acquired quite rapidly, particularly with the use of short repetition time (TR) periods. The complicated frequency response of the magnitude SSFP signal, "transitions zones" and "passbands" every 1/(2TR), implies that the usual mechanisms affecting signal intensity changes will exhibit different sensitivities in these two regimes. Thus frequency shifts *and* changes in the widths of the inherent frequency distributions, widths responsible for so-called reversible relaxation (4), should be accounted for when attempting to adequately model fMRI related signal changes in SSFP. We have derived analytic expressions for the SSFP signal which explicitly account for longitudinal and irreversible transverse relaxation rates, R_1 and R_2 respectively, as well as the central frequency w_o, and width parameter R_2' associated with frequency distributions responsible for reversible relaxation. The sum of R_2 and R_2' is the usual transverse relaxation rate of gradient echo EPI sequences R_2* (4). The expressions derived allow for separate evaluation of the effects of reversible R_2' vs irreversible R_2 transverse relaxation on fMRI related signal changes over the full 1/(2TR) frequency response.

Methods: SSFP images during 30 second blocks of ON/OFF motor activation (finger tapping) were acquired at 3 T (Siemens, TRIO) using a 70^o flip angle, 5 ms TR and echo time of 2.5 ms. For one experiment, passband conditions were obtained over the entire slice with proper shimming while in a second experiment transition zones were introduced by applying a linear shim gradient in the A to P direction (see Fig. 1). Analytic expressions for the SSFP complex signal for three separate frequency distribution (Lorentzian, Gaussian and square) were derived in a manner similar to that used by Ma and Wehrli for the spin echo sequence (4) but with a mathematical series expansion distinct from the double sum expression originally described by Gyngell (5) for SSFP analyses of distribution effects. Our expansion allows for a closed form solution for the Lorentzian distribution, similar to that found by Ganter (6) by other means, and single summation, rapidly converging solutions for the Gaussian and square distributions.

Results: Figure 1 displays experimental fMRI results obtained from a voxel in motor cortex (blue box) elicited under full passband conditions (left panel) and a voxel near a transition zone (right panel). Note that the response in the latter appears somewhat larger than in the former. Figure 2 shows simulations of the SSFP magnitude frequency response (top plot) based on the pulse sequence parameters employed in the experiments and for brain parenchyma tissue parameters $R_1 = 1\ s^{-1}$, $R_2 = 10\ s^{-1}$, and $R_2' = 5\ s^{-1}$ (4) as calculated with Lorentzian, Gaussian and square frequency distributions. No discernible difference between the distributions is observed, though clearly small changes in w_o will cause substantial SSFP signal change even with the inclusion of frequency distribution width effects via R_2'. The signal sensitivity to the reversible relaxation rate R_2' was small (~1%) over the 3 to 7 s^{-1} range regardless of the w_o offset, though at larger TR periods (50 vs 5 ms) the R_2' sensitivity over the same range increased to ~14%. In contrast, even with 5 ms TR's, substantial drops in signal intensity are observed as the irreversible relaxation rate R_2 ranges from 8 to 12 s^{-1} at 100 Hz (40% drop), 50 Hz (44% drop) and 25 Hz (48% drop) offsets from the transition zone (lower plots in Figure 2).

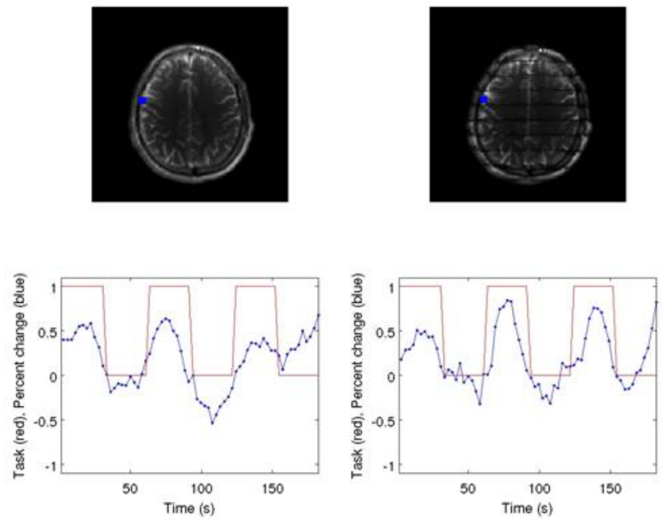

Figure 1: Experimental demonstration of percent signal change of the SSFP signal activation from an ROI associated with the motor cortex (blue square in images) in passband conditions (left) and close to a transition band (right). Somewhat larger fluctuations in the transition band experiments are observed.

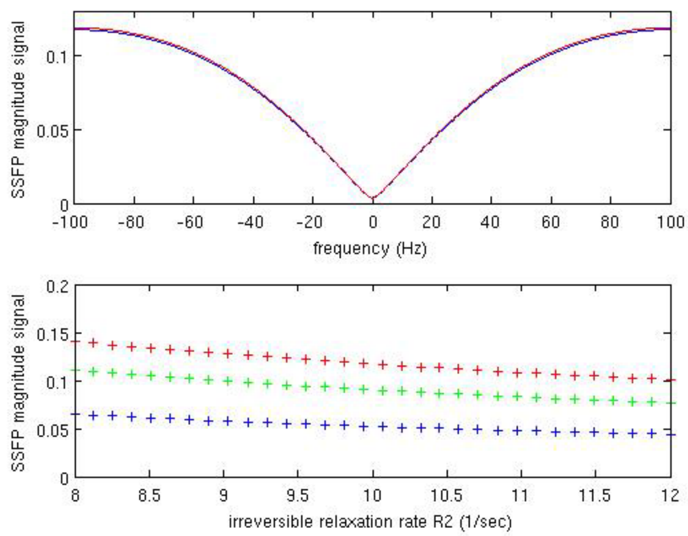

Figure 2: Simulations of the frequency dependence (top) for the SSFP parameters used in our experiment for brain parenchyma ($R_1 = 1\ s^{-1}$, $R_2 = 10\ s^{-1}$, $R_2' = 5\ s^{-1}$) as calculated for Lorentzian (blue), Gaussian (green) and square (red) distributions. The R_2 sensitivity (bottom) at 25 Hz (blue), 50 Hz (green) and 100 Hz (red) from the transition zone over the range 8 to 12 s^{-1} range as calculated with $R_1 = 1\ s^{-1}$ and $R_2' = 5\ s^{-1}$ and with the Lorentzian distribution formuale.

Discussion: Although both early (5) and later (6) literature on SSFP have included discussions of frequency distributions, explicit analytic expressions for specific distributions have either been lacking or in formats difficult to deploy. We applied the reversible vs irreversible transverse relaxation formalism employed by Ma and Wehrli for the spin echo sequence (4) to the SSFP sequence. We also employed a mathematical series expansion previously unnoted for this application and derived straightforward expressions from which the separate effects of irreversible and reversible (frequency distribution) relaxation effects in SSFP were readily simulated. Our preliminary simulations demonstrate that for short TR periods, changes in irreversible relaxation will cause considerably larger SSFP signal intensity modulations than changes in reversible relaxation (frequency distribution widths), a finding that can be incorporated into more sophisticated models and experiments designed to explain the complicated SSFP response to neural activation.

References: (1) Scheffler et al., *NMR Biomed* 2001;14:490-496. (2) Miller et al., *Magn Reson Med* 2003;50:675-683. (3) Lee et al., *Magn Reson Med* 2008;59:1099-1110. (4) Ma and Wehrli, *J Magn Reson B* 1996;111:61-69. (5) Gyngell, *J Magn Reson* 1989;81:474-483. (6) Ganter, *Magn Reson Med* 2006;56:687-691.